Spatial-dispersion effects in a mixed mode of exciton polaritons in CdS

M. V. Lebedev, V. G. Lysenko, and V. B. Timofeev

Institute of Solid State Physics, Academy of Sciences of the USSR
(Submitted 14 November 1983)
Zh. Eksp. Teor. Fiz. **86**, 2193–2200 (June 1984)

The behavior of the refractive index in the region of the A-exciton resonance in CdS has been determined from the deflection of light by a thin prismatic crystal. The transition from the case in which spatial dispersion is important to the case of classical crystal optics has been followed during excitation of the mixed mode. Theory is compared with experiment, and the basic characteristics of the polariton branches are determined.

1. INTRODUCTION

We report here a study of the dispersion properties of a mixed polariton mode in the particular case of the $A_{n=1}$ exciton ground state in hexagonal cadmium sulfide crystals. We know that a mixed mode can be excited in an anisotropic medium and that it is a light-exciton wave whose wave vector makes some angle $\varkappa$ ($0<\varkappa<90°$) with the electric field (see Ref. 1, for example). Such a mode is thus not purely longitudinal ($\varkappa = 0°$) or purely transverse ($\varkappa = 90°$). In the particular case of a mixed mode it is possible in principle to follow the changes in the dispersion properties of exciton polaritons by making a smooth transition, at a fixed value of the damping constant Γ ($T = \text{const}$), from the region in which spatial-dispersion effects are important to the limit corresponding to classical crystal optics. This problem can be solved experimentally by studying the dispersion of the refractive index in the vicinity of an exciton resonance, by observing the refraction of light by a thin prismatic crystal. By varying the angle between the hexagonal axis of the crystal and the electric vector of the incident light wave in this case, one can change the projection of the dipole moment of the transition to the exciton state and thus change the splitting of the upper and lower polariton branches (we will call this splitting the "effective longitudinal-transverse splitting" Δ_{LT}^{*}). The method of light refraction in a thin prism, which was first used in Ref. 2 to construct polariton curves, has certain advantages over interference methods for studying the behavior of the refractive index near exciton resonances.[3,4] The most important of these advantages is that dead-layer effects can be avoided, while they absolutely must be taken into account in the interference methods.[3] We might also note that in working with a mixed polariton mode one can follow the behavior of the refractive index well into the exciton-absorption region, despite the rather large thickness of the sample.

2. CRYSTALS AND EXPERIMENTAL PROCEDURE

In the experiments we used scaly CdS single crystals grown by the Froerichs methods from the gas phase. We selected wafers with a wedge-shaped cross section. The wedge shape is a consequence of the natural although uncontrollable growth. At crystal thicknesses of 10–20 μm the refraction angle at the vertex of the wedge was on the order of 10^{-2} rad. The C_6 hexagonal axis lay in the plane of the wafer and ran parallel to the refracting edge of the wedge, as shown in Fig. 1. The quality of these crystals was quite high. From the line intensities I_1 and I_2 of the exciton-impurity complexes at liquid-helium temperature we conclude that the concentration of residual electrically active impurities did not exceed 10^{15} cm^{-3}. The samples were immersed directly in superfluid helium in an optical cryostat ($T = 1.8$ K). By rotating a shaft on which the samples were mounted we were able to vary the angle (θ) at which light was incident on the surface of the crystal [θ is the angle between the normal to the surface of the crystal and the direction of the incident ray in the plane perpendicular to the principal cross section of the prism (Fig. 1)].

The angle (φ) through which a parallel light beam is deflected by the prism is determined unambiguously by the refraction angle of the prism (α), the angle of incidence (θ), and the refractive index of the prism material (n). In the general case in which the incident beam does not lie in the plane of the principal cross section, the quantities φ, α, θ, and n are related by a rather complicated expression (see Ref. 5, for example). For a thin wedge, in contrast, the simple approximation $\varphi \approx \alpha\,(n-1)$ is quite accurate.

We used the same equation to calculate the refraction angle of the wedge (α) for a sample with dimensions of 1.5 mm, 5 mm, and a thickness of 20 μm, which we used for the

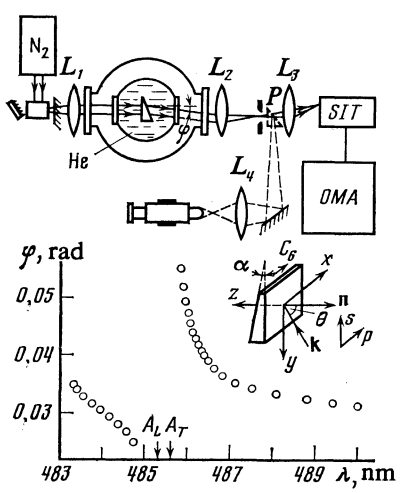

FIG. 1. Experimental apparatus and geometry.

 0038-5646/84/061277-05$04.00

experiments reported below. For this calculation we measured the deflection angle φ, and we adopted $n = 3$ at the wavelength $\lambda = 4884.4$ Å, in accordance with the results of Ref. 2. The value found for α is 0.012 rad.

Figure 1 shows a block diagram of the experimental apparatus. The light source is a tunable laser whose active medium is a dioxane solution of the organic dye coumarin-152A. This laser was pumped by a pulsed nitrogen laser. The use of a laser instead of an incoherent light source fundamentally improves the accuracy of the refractive-index measurements. The power level of the tunable pulse was about 100 W at a length of 6 ns and a spectral width of about 0.5 Å. Experiments were carried out at power densities below 1 kW/cm^2, at which nonlinear changes in the dispersive properties of the medium could be ignored. The laser beam was collimated by a lens L_1 and directed to the crystal. The beam deflected by the crystal was focused to a spot 25 μm in size in the focal plane of lens L_2 ($f = 180$ mm). The displacement of this spot was monitored visually with a measuring microscope (with a rotating prism P in place) or photoelectrically, by projecting an image of the spot (by lens L_3; the rotating prism is not in place in this method) onto the light-sensitive matrix (SIT) of an optical multichannel analyzer (OMA-2). Large deflections of the spot could be measured quite accurately by the visual method. However, it turned out to be absolutely necessary to use the OMA-2 analyzer to study the behavior of the refractive index for the mixed mode of exciton polaritons at small angles of incidence, $\theta \sim 0°$ to 5°. At such small angles θ the deflection angle φ must be measured more accurately, since the changes in the refractive index with the frequency are small in this case. The photoelectric measurement method made it possible to measure the shape of the spot. As a result, we were able to determine the position of the spot maximum more accurately and thus reduce the relative measurement error. While the error in the measurements of the angle by the visual method was $\pm 7 \cdot 10^{-5}$ rad, that in the measurements with the OMA-2 was $\pm 1.5 \cdot 10^{-5}$ rad. Another factor making the photoelectric method convenient is that the transmission of the crystal can be measured at the same time as the spot displacements.

The inset in Fig. 1 shows some representative measurements of the angular deflection of a parallel light beam due to the dispersion of the refractive index in the vicinity of the $A_{n=1}$ exciton resonance of CdS. The arrows mark the known positions of the transverse (A_T) and longitudinal (A_L) excitons. These measurements were carried out with light incident normally on the crystal ($\theta = 0°$) in the polarization $E \perp C_6$. The size of the circles in Fig. 1 indicates the experimental error in the measurement of the angular deflection of the spot and the wavelength spread of the light source. In converting the wavelength to a frequency we made corrections for the refractive index of air in all cases.

3. RESULTS AND DISCUSSION

We studied the dispersion of the refractive index for the transverse and mixed polariton modes in the vicinity of the $A_{n=1}$ exciton resonance. In the discussion below we will need expressions for the diagonal components of the dielectric tensor in the spectral region of interest and for the experimental geometry in Fig. 1. For the longitudinal components $\varepsilon_{xx} \equiv \varepsilon^{\parallel}(\mathbf{E} \| C_6)$ and the transverse component $\varepsilon_{yy} \equiv \varepsilon^{\perp}(\mathbf{E} \perp C_6)$ we have, respectively,

$$\varepsilon^{\parallel} = \varepsilon_0^{\parallel}, \tag{1}$$

$$\varepsilon^{\perp} = \varepsilon_0^{\perp} + \frac{A_0}{\omega_0 + {}^1/_2\hbar\omega^2 c^{-2}[n^2/M_{\perp} + \sin^2\theta\,(1/M_{\parallel} - 1/M_{\perp})] - \omega - i\Gamma}. \tag{2}$$

The second term on the right in (2) is the contribution of the $A_{n=1}$ exciton to the dielectric constant. The quantity A_0 is proportional to the oscillator strength of the phototransition f:

$$A_0 = (2\pi e^2/\omega_0 m_0) Nf, \tag{3}$$

where e and m_0 are the charge and mass of an electron in vacuum, ω_0 is the resonant frequency of the transverse $A_{n=1}$ exciton, and N is the number of unit cells per unit volume of the crystal. The quantities Γ, $M_{\parallel}$, and $M_{\perp}$ in (2) are the exciton damping constant and the longitudinal and transverse translational masses of the exciton. The polariton wave vector $\tilde{\mathbf{k}}$ has been replaced in (2) by the refractive index n, in accordance with the definition $n^2 = c^2\tilde{k}^2/\omega^2$. A dispersion relation for a mixed mode of exciton polaritons can be written[1]

$$\varepsilon^{\perp}\varepsilon^{\parallel} = (\varepsilon^{\perp}\cos^2\delta + \varepsilon^{\parallel}\sin^2\delta)\, c^2\tilde{k}^2/\omega^2 = \varepsilon^{\perp}(n^2 - \sin^2\theta) + \varepsilon^{\parallel}\sin^2\theta, \tag{4}$$

where the angle δ is the angle which the polariton wave vector $\tilde{\mathbf{k}}$ makes with the z axis (according to the experimental geometry, θ and δ are related by Snell's law, $\sin\theta = n\sin\delta$). We will discuss separately the cases in which the wave incident on the crystal was polarized perpendicular to the plane of incidence (the case of s polarization) and in the plane of incidence (p polarization).

We begin with the s polarization. In this case we are dealing exclusively with transverse polariton modes since the electric vector is perpendicular to the C_6 axis. The dispersion relation for transverse exciton polaritons is given by (2). Solving this equation, we find the well-known Pekar equations,[6] which give the frequency dependence of the refractive indices n^+ and n^- for the lower and upper polariton modes. From (2) we see how a change in the angle θ affects the behavior of the refractive index. The only quantity in this expression which depends on the angle θ is the translational mass of the exciton. The effect of the anisotropy of the translational mass turns out to be extremely weak, however. Since n takes on values roughly between 2 and 5 in the present experiments, the first term in square brackets in (2) is about an order or magnitude greater than the second. This assertion is supported by experimental observations of the dispersion of the refractive index in the s polarization at various angles of incidence θ (Fig. 2). We see that in this polarization the experimental dispersion curves for the different values of θ essentially coincident within the experimental errors. The theoretical curves calculated for various angles θ also coin-

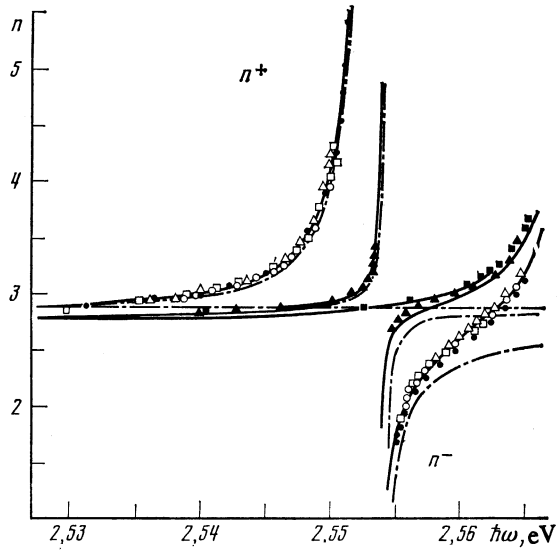

FIG. 2. Behavior of the refractive index near the line of the $A_{n=1}$ exciton. For the s polarization: ●—$\theta = 0°$; ○—$\theta = 21°$; △—$\theta = 41°$; □—$\theta = 56°$. For the p polarization: ■—$\theta = 0°$; ▲—$\theta = 56°$. The dot-dashed curves are theoretical curves calculated without consideration of the B exciton, while the solid curves show calculations incorporating the B exciton. These curves coincide for the n^+ branches.

cide. The dot-dashed lines in Fig. 2 shows calculations for the n^+ and n^- branches of transverse polaritons according to the Pekar equations with the following parameter values: $\varepsilon_0^\perp = 7.4 \pm 0.3$, $A_0 = 16.3 \pm 0.5$ meV, $M_\perp = (0.7 \pm 0.3)m_0$, $\hbar\omega_0 = 2.5519 \pm 0.0002$ eV, $\Gamma = 0$, and $M_\parallel = 5m_0$. The resonant frequency of the transverse polaritons, ω_0, is not an adjustable parameter in this case; it is found from the familiar relation $\omega_L - \omega_0 = A_0/\varepsilon_0^\perp$. The energy of a longitudinal exciton was found experimentally in a study of a mixed polariton mode (more on this below); its value is $\hbar\omega_L = 2.5541 \pm 0.0002$ eV. Furthermore, a variation of $M_\parallel$ has essentially no effect on the shape of the dispersion curve, so we did not treat $M_\parallel$ as an adjustable parameter; we adopted the value $M_\parallel = 5m_0$ in all the calculations, in accordance with data from the literature.[7] In the calculations of the dispersion of the refractive index of the transverse polariton the damping was set at $\Gamma = 0$ in view of the large longitudinal-transverse splitting $\Delta_{LT} = \omega_L - \omega_0 = 2.2$ meV. From measurements of the transmission curves in the case of a mixed polariton mode (as discussed below) we found $\Gamma = 0.02$ meV (i.e., $\Gamma \ll \Delta_{LT}$) for the damping. Consequently, in comparing theory and experiment for the transverse polaritons we are essentially dealing with only three adjustable parameters: $\varepsilon_0^\perp$, A_0, and $M_\perp$. It can be seen from Fig. 2 that a theoretical approximation based on dispersion relation (2) agrees reasonable well with experimental data on the lower transverse polariton branch, while for the upper branch there are substantial discrepancies. The reason for these discrepancies is that higher-energy exciton states, primarily the $B_{n=1}$ exciton, have been ignored. To take these states into account we must add terms $B_0^\parallel/(\omega_0^B - \omega)$ and $B_0^\perp/(\omega_0^B - \omega)$ to expressions (1) and (2), respectively, for the dielectric constant; here ω_0^B is the resonant frequency of the $B_{n=1}$ exciton, and the parameter B_0 is, by analogy with A_0, related to the oscillator strength of the optical transition to the state of the $B_{n=1}$ exciton.

Far from the B-exciton resonance we ignore the damping and the spatial dispersion for the B exciton. In this case, strictly speaking, we would have to solve the dispersion relation for the transverse polariton mode, (2), again, with a dielectric constant incorporating the additive contribution of the B exciton. However, we can use the old expressions for the refractive indices n^+ and n^-, replacing $\varepsilon_0^\perp$ in them by $\varepsilon_0^\perp + B_0^\perp/(\omega_0^B - \omega)$. This approximation is valid if $B_0^\perp/(\omega_0^B - \omega) \ll \varepsilon_0^\perp$ or $\Delta_{LT}^B/(\omega_0^B - \omega) \ll 1$ (Δ_{LT}^B in this condition is the longitudinal-transverse splitting for the B exciton). In the actual frequency interval near the A-exciton resonance this inequality holds, so that this approximation is valid. The B exciton was taken into account in the calculations shown by the solid curves in Fig. 2; the parameters of this exciton were taken from Ref. 2: $\hbar\omega_B = 2.5680$ eV and $B_0^\perp = 2\pi\alpha_B\omega_0^B = 10.3$ meV. The parameters of the A exciton were taken to be the same as before. We see that after the B exciton is taken into account the discrepancy between theory and experiment essentially disappears.

We turn now to the results obtained for the p polarization. In this case we are dealing with a mixed polariton mode. The behavior of the refractive index for this mode is easily found from the solution of dispersion relation (4), but we will not reproduce the very lengthy expression here. Figure 2 shows measurements of the dispersion of the refractive index in the p polarization carried out for angles of incidence $\theta = 0°$ and $\theta = 56°$. The dot-dashed curves are theoretical curves calculated without consideration of the B exciton, as in the case of the transverse polariton mode, while the solid curves incorporate the B exciton (by analogy with the calculations for the transverse mode). The only new parameter in these equation is the quantity $\varepsilon_0^\parallel$, which we were forced to set equal to 8.4 when the B exciton was ignored. In calculations incorporating the B exciton, on the other hand, we found $\varepsilon_0^\parallel = \varepsilon_0^\perp = 7.4$ ($B_0^\parallel = 2\pi\alpha_B^\parallel\, \omega_0^B = 12.8$ meV; Ref. 2). All the other parameters were taken to be the same as before. The difference between $\varepsilon_0^\parallel$ and $\varepsilon_0^\perp$ in the simple model which does not explicitly incorporate the B exciton is therefore due to the approximate nature of this model, and the discrepancy disappears when we incorporate in the dielectric-constant terms describing the B exciton. The dispersion of the refractive index measured in the p polarization for $\theta = 0°$ is due exclusively to the B exciton.

The parameters characterizing the A and B excitons must satisfy simultaneously a large number of dispersion curves of the refractive index which have been measured for the case of a mixed polariton mode at various angles of incidence. As a consequence, the determination of these parameters is more reliable than that in Ref. 2. Figure 3 shows corresponding curves measured at relatively large values of θ, at which damping can still be ignored. With decreasing θ the dispersion curves of n^+ and n^- move closer together; in other words, there is a decrease in the effective longitudinal-transverse splitting. We conclude from Fig. 3 that there is a good agreement between theory and experiment; the values of the adjustable parameters are the same as in Fig. 2.

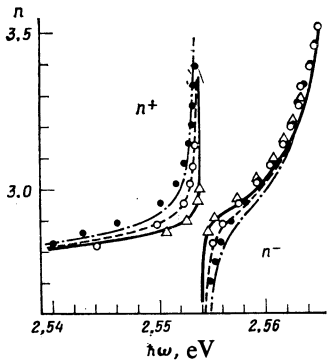

FIG. 3. Frequency dependence of the refractive index of the mixed mode for various angles of incidence θ (the points are experimental, and the curves are theoretical). ● and dot-dashed curves—$\theta = 56°$; ○ and dashed cruves—$\theta = 36°$; △ and solid curve—$\theta = 16°$.

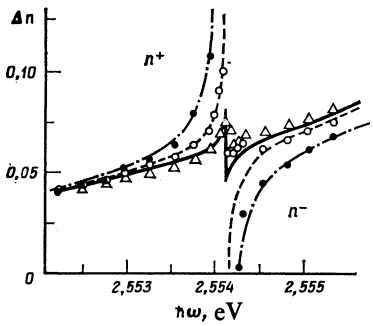

FIG. 4. Behavior of the refractive index of the mixed mode at small angles θ (the points are experimental, and the curves are theoretical). ● and dot-dashed curves—$\theta = 9.5°$; ○ and dashed curves—$\theta = 5°$; △ and solid curves—$\theta = 2.5°$. Plotted along the ordinate is the relative change in the refractive index, $\Delta n = n(\omega) - n(2.5522\text{ eV}) + 0.041$. As we go from $\theta = 5°$ to $\theta = 2.5°$ there is a radical change in the frequency dependence of the refractive index: The discontinuity disappears, and a region of anomalous dispersion appears.

We turn now to the behavior of the refractive index in the mixed mode at small angles of incidence θ, at which the exciton damping Γ begins to have an important effect on the shape of the curves. It follows from the calculations that at $\Gamma = 0$ and at an arbitrarily small but nonzero value of θ there is always a discontinuity on the curve of the refractive index at the transition from the n^+ branch to the n^- branch. If $\Gamma \neq 0$, on the other hand, then a common continuous curve appears for the refractive index beginning at some quite small value of θ corresponding to the value of the damping Γ. The situation here is analogous to the transition to classical crystal optics, which is observed in the transverse mode of exciton polaritons with increasing Γ (Refs. 8 and 9). Figure 4 shows the behavior of the refractive index in the mixed mode at small angles θ. At $\theta = 9.5°$ and $\theta = 5°$ there is a clearly defined discontinuity on the frequency dependence of the refractive index. Experimentally this discontinuity is seen as a rapid decrease in the intensity of the spot in the focal plane of lens L_2 when a certain frequency is reached, while another spot appears simultaneously at a different plane. In other words, there is an abrupt transition from one branch of the refractive index to the other. Under our experimental conditions we were not able to observe two waves simultaneously at the same frequency. In order to observe two waves it would apparently be necessary to use thinner prismatic crystals. The shape of the dispersion curves measured at $\theta < 9.5°$ cannot be described satisfactorily without considering damping. The value of the damping Γ was determined by measuring transmission curves of the crystal in the vicinity of the $A_{n=1}$ exciton resonance and then approximating the experimental curve by a theoretical curve calculated from the solution of dispersion relation (4). For a given value of Γ the imaginary parts of the refractive indices n^+ and n^- are found from the corresponding solution; with this information and the known thickness of the crystal it is then possible to calculate a transmission curve and then compare it with the corresponding experimental curve. As a result of this approximation of the transmission curves measured for angles of incidence equal to 5° and 2.5° we found the best agreement between theory and experiment with the value $\Gamma = 0.02$ meV, in approximate agreement with the values in the literature[3,10] for $T = 1.8$ K. For all the dispersion curves in Fig. 4 the calculations incorporated the B exciton and used the damping value $\Gamma = 0.02$ meV found above. The other adjustable parameters were left unchanged.

At $\theta = 2.5°$ the discontinuity on the frequency dependence of the refractive index disappears (Fig. 4). The spot shifts in first one direction and then another, tracing out the region of the anomalous dispersion of the refractive index. We see from Fig. 4 that the transition to classical crystal optics observed experimentally is described well by the theory, which predicts a classical frequency dependence of the refractive index for $\theta = 2.5°$.

We should also point out that the reason for the discrepancy which remains between theory and experiment on the behavior of the refractive index at $\theta = 5°$ (Fig. 4) is still unclear (see also Ref. 2). Since it is at $\theta = 5°$, i.e., at the transition to the classical dispersion curve, where this discrepancy is observed it may be that its explanation will require a more careful analysis of the behavior of the refractive index near this transition.

A few comments are in order regarding the experimental determination of the frequency of the longitudinal exciton, since we used the value found for ω_L in all the calculations. As the angle θ approaches zero, the frequency interval in which the refractive index for the mixed mode differs substantially from the background value $\sqrt{\varepsilon_0^{\parallel}}$ decreases. At $\theta = 0°$ it contracts to a point, thereby defining a limiting frequency ω^*. It can be shows that this frequency agrees with the frequency of a longitudinal exciton whose wave vector is equal to the wave vector of light in the crystal: $\tilde{k} = (\omega^*/c)\sqrt{\varepsilon_0^{\parallel}}$. To find the frequency (ω_L) of a longitudinal exciton at $\tilde{k} = 0$ we must subtract from $\hbar\omega^*$ the kinetic energy of the exciton, $\hbar^2\tilde{k}^2/2M_{\perp} = \hbar^2\omega^{*2}\varepsilon_0^{\parallel}/2M_{\perp}c^2 \approx 10^{-2}$ meV—which lies within the error of the present experiments. We are thus justified in concluding that we have $\hbar\omega_L = \hbar\omega^* = 2.5541$ eV.

4. CONCLUSION

The experimental method based on the refraction of light by a thin prismatic crystal is thus an effective tool for

studying the single-particle spectrum of exciton polaritons in the particular case of uniaxial cadmium sulfide crystals. In the case of a mixed polariton mode it is possible to controllably change the projection of the dipole moment of the transition to the corresponding exciton state, and thus change the effective longitudinal-transverse splitting ($\Delta^{*}_{LT} \in (\Delta_{LT}, 0)$), by varying the angle between the electric vector of the incident monochromatic wave and the hexagonal axis of the crystal. In the experiments described here the crystal temperature was held constant and low enough that the fixed value of the damping of the exciton polaritons, found from the transmission spectra, satisfied the condition $\Gamma \ll \Delta_{LT}$. This condition ultimately made it possible to follow the changes in the dispersion properties of the mixed mode in a smooth transition from the region in which spatial dispersion is important ($\Gamma \ll \Delta^{*}_{LT}$) to the limit corresponding to classical crystal optics ($\Gamma \sim \Delta^{*}_{LT}$). The dispersion properties of the mixed mode can be described quite well analytically over the entire range of the longitudinal-transverse splitting, and the parameters characterizing the single-particle polariton spectrum (ε_0, $M_\perp$, and A_0) can be determined. It appears that the refraction of light by a thin prismatic crystal could also be used effectively to study the nonlinear dielectric properties of a medium near exciton resonances.

[1]S. A. Permogorov, V. V. Travnikov, and A. V. Sel'kin, Fiz. Tverd. Tela (Leningrad) **14**, 3642 (1972) [Sov. Phys. Solid State **14**, 3051 (1973)].
[2]I. Broser, R. Broser, E. Backmann, and E. Birkicht, Solid State Commun. **39**, 1209 (1981).
[3]I. V. Makarenko, I. N. Uraltsev, and V. A. Kiselev, Phys. Status Solidi **b98**, 773 (1980).
[4]M. S. Brodin, N. A. Davydova, and M. I. Strashnikova, Pis'ma Zh. Eksp. Teor. Fiz. **19**, 567 (1974) [JETP Lett. **19**, 297 (1974)].
[5]A. I. Tudorovskiĭ, Teoriya opticheskikh priborov (Theory of Optical Instruments), Vol. 1, Izd, Akad. Nauk *SSSR*, Leningrad-Moscow (1948), p. 122.
[6]S. I. Pekar, Zh. Eksp. Teor. Fiz. **33**, 1022 (1957) [Sov. Phys. JETP **6**, 785 (1958)].
[7]J. J. Hopfield and D. G. Thomas, Phys. Rev. **122**, 35 (1961).
[8]A. S. Davydov and E. N. Myasnikov, Phys. Status Solidi **b63**, 325 (1974).
[9]M. I. Strashnikova and E. V. Bessonov, Zh. Eksp. Teor. Fiz. **74**, 2206 (1978) [Sov. Phys. JETP **47**, 1148 (1978)].
[10]I. Broser, M. Rosenzweig, R. Broser, M. Richard, and E. Birkicht, Phys. Status Solidi **b90**, 77 (1978).

Translated by Dave Parsons